Triple Helix Formation by (G,A)-Containing Oligonucleotides: Asymmetric Sequence Effect†

Paola B. Arimondo,‡ Francisca Barcelo,§ Jian-Sheng Sun,*,‡ Jean-Claude Maurizot,|| Thérèse Garestier,‡ and Claude Hélène‡

Laboratoire de Biophysique, Muséum National d'Histoire Naturelle, INSERM U201, CNRS URA 481, 43 rue Cuvier, 75231 Paris Cedex 05, France, Departemeto de Biologia i Ciències de la Salut, Universitat de les Illes Balears, Palma de Mallorca, Spain, and Centre de Biophysique Moléculaire, Université d'Orléans, rue Charles Sadron, 45071 Orléans Cedex 2, France

Received March 11, 1998; Revised Manuscript Received September 14, 1998

ABSTRACT: Sequence effects on the stability of purine-motif (also called (G,A)-motif) triple helix have been investigated through two symmetry-related systems: one of them had a 5′(GGA)$_4$3′ core sequence of triplex-forming oligonucleotides (TFOs), whereas the other one had a reversed 5′(AGG)$_4$3′ core sequence. These (G,A)-containing TFOs were prone to self-associate into intermolecular complexes at room temperature. The competition of TFOs' self-association with triple helix formation was assessed, and minimized. By varying the lengths and the terminal base sequences of TFOs, the following were found that (1) The stability of two triple helices with identical length and base composition but reverse strand orientation may be significantly different (up to a factor of 6). (2) When the 5′(GGA)$_4$3′ core sequence was extended at the 3′-end by a G, the 13-nt TFO exhibited 3- and 5-fold higher affinity toward the target double-stranded DNA (dsDNA) than the longer 14-nt and 15-nt TFOs in which one and two A(s) were added at the 3′-end of the 13-nt TFO, respectively. In contrast, when the similar extensions occurred at the 5′-end of the 5′(AGG)$_4$3′ core sequence, the length increase provided a higher binding affinity of TFOs toward the target duplex. (3) The nature of the base triplets involved at the ends of triple helices may have great influence on triplex stability. The observed asymmetric sequence effect of the (G,A)-motif triple helix formation is discussed in terms of the binding strength of the first base triplet(s) at the 3′ end which seems to be deeply involved in the nucleation step of triple helix formation and therefore to be a determining factor for triplex stability.

Triple helices were first observed in 1957 for polyribonucleotides (*1*). These triple-helical complexes suggest an approach to recognize specifically a double-stranded DNA (dsDNA) whereby a short oligonucleotide binds into the major groove of dsDNA by oligonucleotide-directed triple helix formation (*2*, *3*). Triple-helix-forming oligonucleotides (TFOs) can compete with DNA binding proteins (*4*, *5*) and interfere with transcription of a specific gene (*6*−*12*). TFOs have also been used to deliver a site-specific mutation in selected genes, to achieve permanent and inheritable changes in gene expression (*13*−*15*). Oligopyrimidine or oligopurine third strands bind to the major groove of the underlying DNA duplex through either Hoogsteen or reverse Hoogsteen hydrogen bonds, respectively (*16*). In the pyrimidine motif, a (C,T)-containing oligonucleotide binds parallel to the target oligopurine strand through Hoogsteen hydrogen bonds, and forms canonical C·GxC$^+$ and T·AxT base triplets. Due to the requirement for cytosine protonation, the stability of a (C,T)-motif triple helix is pH-dependent. In the purine motif, (G,A)-containing oligonucleotides bind to the oligopurine strand of the duplex by forming C·G*G and T·A*A base triplets through reverse Hoogsteen hydrogen bonds (*17*−*23*). (G,T)-containing oligonucleotides can form triplexes with either Hoogsteen or reverse Hoogsteen hydrogen-bonding interaction and have parallel or antiparallel orientation with respect to the target oligopurine strand sequence, respectively. It has been shown that the preferred strand orientation depends on the sequence of oligonucleotides (*21*, *24*, *25*). The formation of both (G,A)- and (G,T)-motif triple helices is pH-independent but requires the presence of divalent cations in the millimolar concentration range.

It has been reported that the (G,A)-motif triplex can be very stable (*26*−*32*). However a G-rich third strand is prone to form inter- or intramolecular self-associated structures involving the formation of G-quadruplex, (G,A)-parallel duplex, or hairpin structures. Such structures which are stabilized by physiological concentrations of cations suggest that self-association could take place in vivo. As a result, the ability of a (G,A)-containing TFO to bind to its intended

† This work has been supported in part by the Università degli Studi di Pisa, in part by the European Community TMR grant to P.B.A.

* To whom correspondence should be addressed.

‡ Muséum National d'Histoire Naturelle.

§ Universitat de les Illes Balears.

|| Université d'Orléans.

[1] Abbreviations: bp, base pair (s); nt, nucleotide; ·, Watson−Crick base pairing; x, Hoogsteen or reverse Hoogsteen base pairing; TFO-(s), triplex forming oligonucleotide(s); ssDNA, single-stranded DNA; dsDNA, double-stranded DNA; HEPES, *N*-(2-hydroxyethyl)piperazine-*N*′-(2-ethanesulfonic acid); T_m, melting temperature; UV, ultraviolet; CD, circular dichroism; FTIR, Fourrier transformed infrared spectroscopy; NMR, nuclear magnetic resonance spectroscopy; PAGE, polyacrylamide gel electrophoresis; WC, Watson−Crick.

10.1021/bi9805588 CCC: $15.00
Published on Web 10/30/1998

target is reduced. While the ability of G-rich nucleic acids to be self-associated into various G_4-quadruplexes has been well-characterized by X-ray diffraction of single crystals and by NMR spectroscopy (*33*−*35*), the other self-associations are only beginning to be understood. In general, the observed complexes are stabilized by Mg(II) in a sequence-dependent manner. Different intermolecular structures have been proposed and characterized by NMR, FTIR, UV, and Raman spectroscopies, footprinting analysis, PAGE, and pyrene excimer fluorescence (*36*−*47*). These complexes are sensitive to pH when the protonation of adenine (A^+) are involved, to ionic strength, in particular to Mg(II) concentration, and can be interconvertible. Therefore, different structures may be involved for the different sequences of (G,A)-containing oligonucleotides ($d(GA)_n$, $d(GGA)_n$, $d(GGGA)_n$) (*48*). These structures depend on the length and the sequence of the oligonucleotide; for instance, $d(GGGA)_n$ oligonucleotides tend to form intramolecular hairpins, whereas $d(GGA)_n$ ones tend to form homoduplexes and hairpins depending on their length (*47*). The absence of Mg(II) seems to favor intramolecular hairpin structures rather than intermolecular homoduplexes (*37*−*39*, *47*).

In the present study, the competition between the self-association of the oligonucleotides containing $(GGA)_n$- and $(AGG)_n$-repeats and the process of (G,A)-motif triple helix formation was first studied. The (G,A)-motif triple helix formation was then investigated under the conditions where self-association of TFOs was negligible. The results obtained stress the importance of the length and the base sequence of the (G,A)-containing oligonucleotides, especially the nature of the bases at the 3′-end of (G,A)-containing third strand oligonucleotides facing the 5′-end of the oligopurine strand of the target DNA duplex.

MATERIALS AND METHODS

Oligonucleotides. Oligonucleotides were purchased from Eurogentec and purified using quick spin columns Sephadex G-25 (Boehringer, Mannheim, Germany). Concentrations were determined spectrophotometrically at 25 °C using molar extinction coefficients at 260 nm calculated from a nearest-neighbor model (*49*).

Oligonucleotide-directed triple-helix formation was investigated using two 31-bp DNA targets: one contains a 15-bp oligopyrimidine·oligopurine tract which is part of the HIV-*nef* gene (located at position 8571−8585), and the other one contains the inverted sequence. Various (G,A)-containing TFOs of different length and base composition were tested.

Gel Retardation Assay. For DNA triplex gel retardation assays, either the purine strand of the 31-bp duplexes or the triplex-forming oligonucleotides were 5′-end-labeled with [γ-^{32}P]ATP (Amersham Arlington Heights, IL) by T4 polynucleotides kinase (New England Biolabs, Beverly, MA). Increasing concentrations (20 nM to 100 μM) of either the TFOs or the corresponding duplex target were added to 10 nM of the labeled duplex or to 20 nM of the labeled triplex-forming oligonucleotide, respectively, in the presence of 10 mM $MgCl_2$, 100mM NaCl, 50 mM HEPES, pH 7.2, 10% sucrose, and 0.5 μg/μL tRNA. The samples were incubated overnight or as indicated at the desired temperature (4−37 °C). Electrophoresis was performed on a nondenaturing 15% polyacrylamide gel containing 10 mM $MgCl_2$ and 50 mM HEPES, pH 7.2 at the incubation temperature.

For single-stranded DNA (ssDNA) gel retardation, 10 nM of 5′ end-labeled triplex-forming oligonucleotide was added to increasing amounts of the corresponding nonradiolabeled oligonucleotide to reach a range of concentrations of 20 nM-100 μM in the presence of 0−10 mM $MgCl_2$ (as indicated), 100 mM NaCl, 50 mM HEPES, pH 7.2, 10% sucrose, and 0.5 μg/μL tRNA with sample incubation at the indicated temperature (4−37 °C), overnight or as indicated. Electrophoresis was performed as described above for triplex gel retardation. The reference oligonucleotide, A_{15}, and the reference duplex, A_{15}·T_{15}, were 5′ end-labeled on the purine strand by T4 polynucleotide kinase using [γ-^{32}P]ATP, and electrophoresed as described for the triplex gel retardation experiments.

Dissociation Constants from Analysis of DNA Gel Retardation Assays. The apparent fraction, Θ, of target duplex bound by oligonucleotide was calculated for each gel lane using the definition:

$$\Theta = S_{\text{triplex}}/(S_{\text{triplex}} + S_{\text{oligonucleotide}}) \quad (1)$$

where S_{triplex} and $S_{\text{oligonucleotide}}$ represent the integration of area of the phosphor signal for the triplex complex and oligonucleotide, respectively. According to a two-state model, the apparent triplex dissociation constant, K_d, is defined as

$$K_d = ([D]\,[O])/[T] \quad (2)$$

$$D + O \underset{K_d}{\rightleftharpoons} T$$

where [D] is the concentration of the duplex, [O] of the TFO and [T] of the triplex. Under our experimental conditions $[O]_0 \ll [D]_0$ (increasing concentrations of duplex [0.02 to 2 μM] are added to 20 nM of triplex-forming oligonucleotide) so the apparent fraction Θ can be calculated using

$$\Theta = [T]/([O] + [T]) = [D]/(K_d + [D]) \quad (3)$$

By least-squares fitting of the data to the binding isotherm of eq 3, values of the apparent triplex dissociation constant, K_d, were obtained.

DNase I Protection Assay for Triplex Formation: The DNA template for the DNase I protection assay on the oligopyrimidine-containing strand of the target was obtained by digestion of pSG-F47 with *Blp*I and labeling with [α-^{32}P]-dTTP in the presence of reverse transcriptase (Boehringer, Mannheim). The labeled plasmid was then digested to completion with *Bbs*I. The radiolabeled duplex was gel purified prior to footprint assays on a native 8% polyacrylamide gel, electroeluted in TBE (89 mM Tris-base, 89 mM boric acid, and 2 mM EDTA). The duplex (40nM) was dissolved in 10 μL of the buffer: 50 mM HEPES pH=7.2, 50 mM NaCl, 10 mM $MgCl_2$, 5 mM $CaCl_2$. Then 6 μM of the TFO 13GA or of the control oligonucleotide (5′ TTCT-TCTTTTTTCT 3′) was added. The mixture was incubated for 12 h at 37 °C. For the DNase I footprint assay, 1 μL of DNase I (Sigma, Germany) was added, and the reaction was performed for 40 s at 20 °C. The reaction was stopped by the addition of 1.5 μL solution containing (EDTA, SDS) and vigorous stirring. After double precipitation in ethanol the samples were resuspended in 95% formamide and heated at

Table 1: Triplex K_d Values of the 31Y/31R and I-31Y/31R Systems[a]

A

5' TFO 3'	5'-TGCGCCCA **CCTCCTCCTCCTCTT** GTGCGCGT-3' **31Y** 3'-ACGCGGGT **GGAGGAGGAGGAGAA** CACGCGCA-5' **31R**	K_D(μM)
12GA	5'- **GGAGGAGGAGGA** -3'	1.5±0.2
13GA	5'- **GGAGGAGGAGGAG** -3'	0.11±0.01
14GA	5'- **GGAGGAGGAGGAGA** -3'	0.35±0.02
15GA	5'- **GGAGGAGGAGGAGAA** -3'	0.51±0.05

B

5' TFO 3'	5'-TGCGCGTG **TTCTCCTCCTCCTCC** ACCCGCGT-3'**I-31Y** 3'-ACGCGCAC **AAGAGGAGGAGGAGG** TGGGCGCA-5'**I-31R**	K_D(μM)
I-12GA	5'- **AGGAGGAGGAGG** -3'	0.28±0.07
I-13GA	5'- **GAGGAGGAGGAGG** -3'	0.14±0.02
I-14GA	5'- **AGAGGAGGAGGAGG** -3'	0.09±0.01
I-15GA	5'- **AAGAGGAGGAGGAGG** -3'	0.08±0.01

[a] Values of K_d were calculated as described in Materials and Methods. The mean value of 3−5 different experiments is reported.

95 °C for 4 min before being loaded onto a denaturing 10% polyacrylamide gel (19:1 acrylamide/bisacrylamide) containing 7.5 M urea in TBE buffer (50 mM Tris base, 55 mM boric acid, 1 mM EDTA).

UV Absorption and Circular Dichroism Spectroscopy. Thermal denaturation and renaturation studies of duplexes and triplexes were carried out on a Kontron Uvikon 940 spectrophotometer with 1-cm optical path length quartz cuvettes. The cell holder was thermoregulated by an 80% water/20% ethylene glycol circulating liquid. Sample temperature was decreased from 80 to 0 °C and increased back to 80 °C at 0.1−0.5 °C/min (as indicated) with absorption readings at 260 and 440 nm taken every 1−1.2 °C. Samples were kept for an additional 30 min at the lowest and highest temperature. All samples were prepared in a buffer containing 10 mM sodium cacodylate, pH 7.0, 100 mM NaCl, and 0−10 mM $MgCl_2$ unless otherwise indicated. For the melting temperature (T_m) analysis, the drift of baseline was corrected by subtracting absorptions at 440 nm from those at 260 nm and plotted against temperature (°C). The maximum of the first derivative d*A*/d*T* was taken as a first estimation of the T_m value.

The CD spectra were recorded with a Jobin Yvon Mark V Dichrograph with 1-cm optical path length quartz cuvettes. Data acquisition and analysis were performed on a microcomputer interfaced to the spectrometer. The temperature of the cell was controlled by a circulating refrigerated water bath. Each CD spectrum was run at least twice, and the possible baseline drifts were checked. Scanning was carried out from 220 to 340 nm at 60 nm/min. All samples were in a buffer containing 10 mM sodium cacodylate, pH 7.0, 100 mM NaCl, and 0−10 mM $MgCl_2$ unless otherwise indicated.

RESULTS

Oligonucleotide-directed triple-helix formation was first investigated using two 31-bp DNA targets containing a 15-bp oligopyrimidine·oligopurine tract (Table 1). The TFOs designed to bind the duplex 31Y/31R differ only at their 3′ end (5′ end of the oligopurine tract of the duplex): 12GA contains four (GGA)-repeats, 13GA contains an additional G at the 3′-end; 14GA and 15GA correspond to 13GA with one or two additional adenine(s) at the 3′ end, respectively. The system of the duplex I-31R/Y has an inverted sequence as compared to the 31Y/31R one. The TFOs I-12GA, I-13GA, I-14GA, and I-15GA have a common $(AGG)_4$ tract and differ at the 5′-end, whereas they share the same sequence at the 3′-end.

Self-Associations of (G,A)-Containing Oligonucleotides. DNA thermal denaturation by UV spectrophotometer and circular dichroism (CD) as well as polyacrylamide gel electrophoresis (PAGE) were used to investigate the self-association of the (G,A)-containing TFOs.

DNA thermal dissociation experiments carried out with the TFOs, 15GA, 14GA, and 13GA, in a 10 mM cacodylate buffer (pH 7.2) containing 100 mM NaCl and 0−10 mM $MgCl_2$ or other salts (LiCl, KCl), exhibited a transition in the 10−30 °C temperature range under all salt conditions, as exemplified by the melting curve of the 15GA (Figure 1A). The melting temperature of the self-associated 15GA was about 18 °C in the presence of 100 mM of monocations ($Li^+/Na^+/K^+$) and was increased up to 30 °C upon addition of 10 mM Mg^{2+}. The absence of hysteresis indicated that the complex formation was fast process as compared to the heating and cooling rates of the samples (1−1.2 °C/min.). The melting curves were concentration-dependent and shifted to higher temperatures at higher concentrations, in agreement with an intermolecular process. It is noted that the change in hypochromicity upon melting of the 15GA was about 10% which was lower than that usually observed in Watson−Crick duplex. This difference may indicate weaker base stacking interactions in the (G,A)-homoduplex than that in WC duplex.

The CD spectrum of the 15GA also showed a self-associated complex which was further stabilized upon addition of 10 mM $MgCl_2$ (Figure 1B). At low temperatures, there was a strong positive peak between 263 nm and a negative peak at 245 nm as has been already observed for $d(GA)_{15-25}$ oligomers (*36*, *41*, *42*). Heating of the 15GA sample led to the disappearance of the positive peak at 263 nm and of the negative peak at 245 nm, and the appearance of a positive peak at 258 nm and a negative peak at 285 nm, characteristic of (G,A)-containing oligonucleotides in a non-self-associated state (*36*). The observed T_m of 30 °C (Figure 1B, insert) was in agreement with that measured under the same experimental conditions from the UV absorption data.

At low temperature (4 °C), a concentration-dependent, step-ladder, abnormal gel mobility was observed by standard PAGE experiments carried out at pH 7.2, in a HEPES buffer (50 mM) containing 100 mM NaCl and 10 mM $MgCl_2$ (Figure 2A). At 60 μM 15GA, a plateau was reached and higher concentrations did not produce any further retarded band on a non-denaturing gel. The band obtained at the plateau had a slightly reduced mobility compared to the reference duplex $A_{15}T_{15}$ (data not shown). These abnormal gel mobilities of (G,A)-containing oligomers indicated that the self-associated intermolecular complexes were formed at low temperature. As temperature was raised from 4 to 37 °C, the self-associated complexes vanished in agreement with the DNA thermal denaturation experiments. The

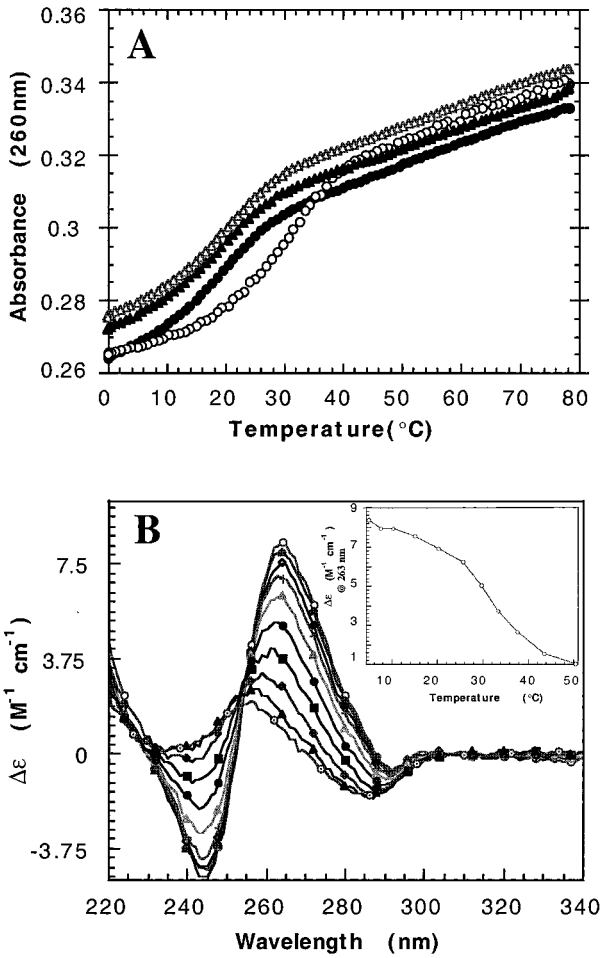

FIGURE 1: Spectroscopic evidences for the self-association of the (G,A)-containing TFOs. (A) UV melting profiles recorded at 260 nm of the 15GA oligonucleotide (5′GGAGGAGGA GGAGAA3′) at 1.5 μM in a buffer containing 10 mM sodium cacodylate (pH = 7.0), and in the presence of 100 mM NaCl (●); 100 mM LiCl (△) or 100 mM KCl (▲), or in the presence of 100 mM NaCl and 10 mM $MgCl_2$ (○). (B) CD spectra of the 15GA oligonucleotide (1.5 μM) in 10 mM sodium cacodylate buffer (pH = 7.0) in the presence of 100 mM NaCl and 10 mM $MgCl_2$ at different temperatures (top to bottom at 263 nm peak): 4.8 °C (○); 7.3 °C (△); 10.2 °C (◆); 15 °C (◇); 20.1 °C (+); 25.6 °C (△); 29.6 °C (●); 33.4 °C (■); 37.6 °C (◆); 43.5 °C (▲); 50.5 °C (⊙). In the insert, variations of $\Delta\epsilon$ (M^{-1} cm^{-1}) at 263 nm are reported as a function of temperature (°C).

association was quite fast, since the same results were obtained by heating the samples 15 min at 90 °C before loading on the gel. The self-associated complexes were much less pronounced in the absence of Mg^{2+} (Figure 2B). The discrete bands with intermediate mobilities between uncomplexed and complexed species were also observed in earlier works (*27*, *36*) for other (G,A)-containing oligonucleotides within the same range of concentrations and under similar experimental conditions. They were presumed to arise from an average mobility between the associated and dissociated species due to dissociation and fast reassociation within the gel.

To determine the stoichiometry of the self-associated complex, the 15GA oligonucleotide (A) was mixed with a 22-nt oligonucleotide (B) in which a T_7 tail was appended at the 5′ end of the 15GA. If equimolar amounts of oligomer A are mixed with B, then the stoichiometry of a given complex can be determined from the number of mixed

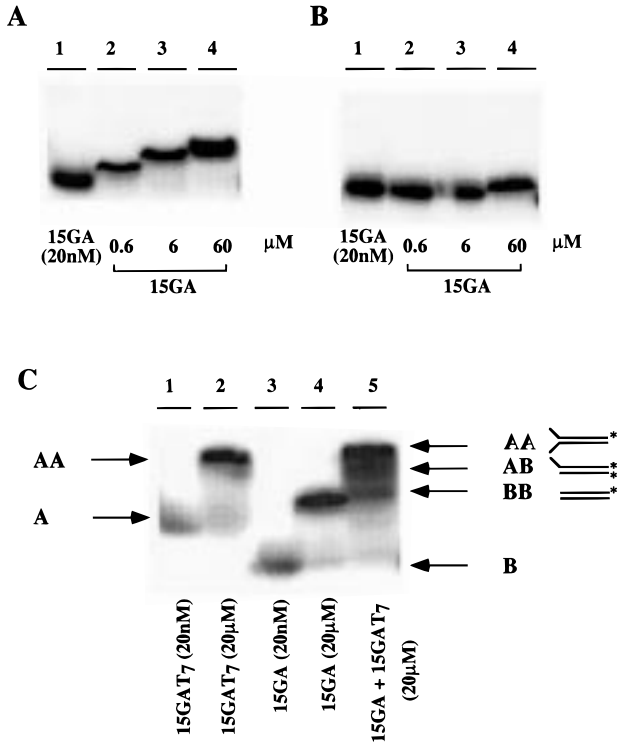

FIGURE 2: Gel retardation assays carried out with the 15GA oligonucleotide in 50 mM HEPES buffer (pH = 7.2) and 100 mM NaCl, in the presence of 10 mM $MgCl_2$ (A) or in the absence of $MgCl_2$ (B), at 4 °C. In each gel, lanes 1−4 correspond to the addition of 0, 0.6, 6, 60 μM of unlabeled 15GA to 20 nM of radiolabeled 15GA oligonucleotide. (C) Mixing experiment carried out with 20 μM 15GA (5′GGAGGAGGAGGAGAA3′) and 20 μM $15GAT_7$ (5′TTTTTTTGGAGGAGGA GGAGAA3′). The gel retardation assay was performed under the same condition as shown in A: lane 1 corresponds to 20 nM of radiolabeled $15GAT_7$; lane 2 to 20 μM of unlabeled $15GAT_7$ added to 20 nM of radiolabeled $15GAT_7$; lane 3 to 20 nM of radiolabeled 15GA; lane 4 to 20 μM of unlabeled 15GA added to 20 nM of radiolabeled 15GA; lane 5 to 20 μM of unlabeled $15GAT_7$ and of unlabeled 15GA added to 20 nM of radiolabeled $15GAT_7$ and of radiolabeled 15GA. **A** indicates the single-stranded oligonucleotide $15GAT_7$; **AA** the dimeric complex of the $15GAT_7$; **B** indicates the single-stranded oligonucleotide 15GA and the dimeric complex of the 15GA; while **AB** indicates the heterodimeric complex formed by the 15GA with the $15GAT_7$.

species that are produced. For example, dimer formation would result in three different complexes resolved on a native gel, the AA, AB, and BB complexes. In Figure 2C, the interaction between 15GA and $15GAT_7$ was studied at two different concentrations. At 20 nM of each oligonucleotide, a single band was observed corresponding to the single-stranded oligonucleotide. At higher concentrations (20 μM) most of the band was converted to a strongly retarded band which corresponds to the self-associated species. When A and B were mixed at high concentration (20 μM) only three complexes were observed, corresponding to the AA, AB, and BB complexes. Therefore the mixing experiments evidenced a dimeric homoduplex formation by 15GA oligonucleotides. A similar behavior was also observed for the other (G,A)-containing oligonucleotides.

Oligonucleotide-Directed Triple Helix Formation. To assess the effect of the concentration-dependent self-association of the TFOs containing (GGA)-repeats on triple helix formation, gel retardation assays were carried out with either

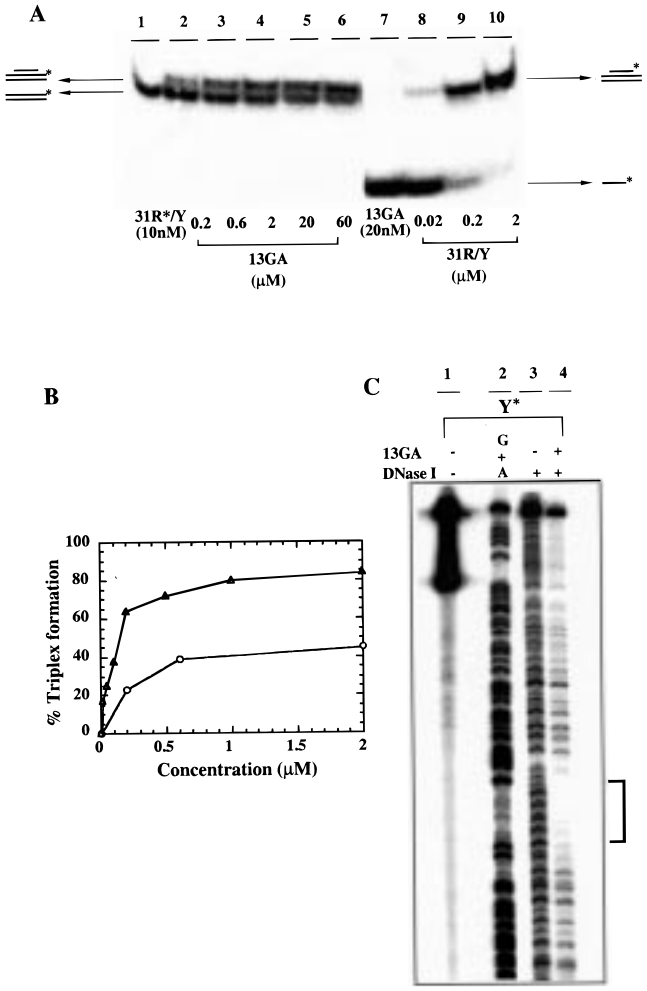

FIGURE 3: Triplex formation of the 13GA toward its target duplex 31Y/31R was investigated by gel retardation assays. (A) Triplexes were formed at 37 °C overnight in 50 mM HEPES buffer (pH = 7.2) and in the presence of 100 mM NaCl and 10 mM $MgCl_2$, by titrating either the TFO 13GA (0, 0.2, 0.6, 2, 20, 60 μM) to 10 nM of radiolabeled target duplex 31Y/31R (lanes 1−6), or the target duplex (0, 0.02, 0.2, 2 μM) to 20 nM of radiolabeled TFO 13GA (lanes 7−10). (B) Quantification of the gel retardation experiments (see above): The titration of the 13GA to 10 nM of the 5′-radiolabeled target duplex 31Y/31R is shown (○), whereas that of the 31Y/31R duplex to 20nM of the radiolabeled 13GA is indicated by △. (C) DNase I footprinting experiment was carried out at 20 °C on the 31Y/31R duplex in the absence and in the presence of the TFO 13GA (lanes 3 and 4, respectively). The DNA was 5′-radiolabeled on the oligopyrimidine-containing strand. Lane 2 is a Maxam−Gilbert G+A sequencing lane. The square brackets indicate the domain of triplex formation.

radiolabeled duplex (labeled at the 5′-end of the oligopurine-containing strand) or 5′-end-radiolabeled TFOs. Nondenaturing electrophoresis was performed in a 50 mM HEPES buffer (pH 7.2) containing 100 mM NaCl and 10 mM $MgCl_2$, at 37 °C. When 10 nM of labeled duplex was titrated with increasing concentrations of TFOs, the retarded band corresponding to the triplex species reached a plateau far below 100% of duplex-to-triplex conversion even at high concentrations of TFOs, as illustrated by the 13GA (Figure 3A, lanes 1−6). This result could not be ascribed to imperfection in the preparation of the target duplex during annealing of two single strands (31Y and 31R) since experiments performed at pH 6.0 with two (C,T)-containing oligonucleotides 15TC (5′CCTCCTCCTCCTCTT3′) and 13TC (5′CCTCCTCCTCCTC3′) with an appropriate parallel orientation with respect to the same target oligopurine sequence did form 100% triplex at high concentration of TFOs (data not shown). In contrast, when experiments were carried out with 20 nM of 5′-end-radiolabeled TFOs and increasing amounts of target duplex, the retarded band approached 100% of triplex formation at high concentrations of duplex (2−5 μM) (Figure 3A, lanes 7−10), and the reproducibility of the data was satisfactory. It has been checked that this difference was held even when 20 nM radiolabeled duplex was used (data not shown). Triplex formation was further confirmed by DNase I protection assays, as the presence of the 13GA bound to the duplex 31Y/31R protected the target duplex against DNase I digestion at 37 °C (Figure 3C).

The discrepancy in the quantitative determination of triplex formation by either duplex or TFO radiolabeling could easily be explained by the self-association of the TFOs containing (GGA)-repeats. This observation infers that a significant amount of TFOs was self-associated in the concentration range compatible with triplex formation. Therefore, only part of the oligonucleotide was present in solution as free single-stranded species and was competent to form triple helices with the target duplex. Consequently, in the present work, the study of (G,A)-containing oligonucleotide-directed triple helix formation was carried out by gel retardation assay under the conditions where the self-association of TFOs was negligible, i.e., by using 20 nM labeled TFOs and increasing concentration of target duplex at 37 °C.

Effect of Sequence and Length. The apparent dissociation binding constant K_d determined from nondenaturing PAGE assays of triplex formation in the first system (31Y/31R, Table 1A) showed that the 13GA's K_d was not only about 10-fold lower than that of the shorter 12GA, but surprisingly also about 3- and 5-fold lower than that of the longer TFOs, 14GA and 15GA, respectively. It has been noted that all these oligonucleotides (12GA, 13GA, 14GA, and 15GA) shared a common 5′-end and differed only in the base sequence at the 3′-end. Only the 13GA has a G at the 3′-end, the other TFOs have at least one A at the 3′-end. This observation strongly indicates a remarkable sequence effect on triplex formation. Therefore, another system was studied where the strand orientation of the target duplex (I-31Y/31R) and that of the TFOs (I-12GA, I-13GA, I-14GA and I-15GA) was reversed as compared to the first system (Table 1).

By doing so, all TFOs shared a common 3′ end and differed only at their 5′ end (Table 1B). As the other (G,A)-containing TFOs studied above, self-association was also observed with these oligomers and the self-associated complexes had thermal stability similar to that of their analogues with opposite polarity (data not shown). The results of the gel retardation assays carried out under similar conditions showed that in this case, longer oligonucleotides formed more stable triple helices than the shorter ones. The apparent K_d value of the longest I-15GA was about 1.8- and 3.5-fold lower than that of the shorter I-13GA and I-12GA TFOs, respectively.

A comparison of these two symmetry-related systems revealed important effect of sequence polarity on triplex stability. For a given length of TFOs, the ones in the second system (I-31Y/31R) exhibited up to 6-fold higher affinity toward the target duplex sequence to form triple helix than

Table 2: Triplex K_d Values of the 31Y/31R and I-31Y/31R Systems[a]

A

5' TFO 3'	5'-TGCGCCCA CCTCCTCCTCCTCTT GTGCGCGT-3' **31Y** 3'-ACGCGGGT GGAGGAGGAGGAGAA CACGCGCA-5' **31R**	K_D (μM)
14GA	5'- GGAGGAGGAGGAGA -3'	0.35±0.02
14TGA	5'- GGAGGAGGAGGAGT -3'	0.2±0.1
14CGA	5'- GGAGGAGGAGGAGC -3'	0.9±0.2
14GGA	5'- GGAGGAGGAGGAGG -3'	0.5±0.2
13GA	5'- GGAGGAGGAGGAG -3'	0.11±0.01

B

5' TFO 3'	5'-TGCGCGTG TTCTCCTCCTCCTCC ACCCGCGT-3'**I-31Y** 3'-ACGCGCAC AAGAGGAGGAGGAGG TGGGCGCA-5'**I-31R**	K_D(μM)
I-14GA	5'- AGAGGAGGAGGAGG -3'	0.09±0.01
I-14TGA	5'- TGAGGAGGAGGAGG -3'	0.11±0.04
I-14CGA	5'- CGAGGAGGAGGAGG -3'	0.10±0.03
14GGA	5'- GGAGGAGGAGGAGG -3'	0.13±0.03
I-13GA	5'- GAGGAGGAGGAGG -3'	0.14±0.02

[a] Values of K_d were calculated as described in Materials and Methods. The mean value of 3−5 different experiments is reported.

Table 3: Triplex K_d Values of the 31CY/31GR and I-31CY/31GR Systems[a]

A

5' TFO 3'	5'-TGCGCCCA CCTCCTCCTCCTCCT GTGCGCGT-3' **31CY** 3'-ACGCGGGT GGAGGAGGAGGAGGA CACGCGCA-5' **31GR**	K_D(μM)
14GA	5'- GGAGGAGGAGGAGA -3'	0.45±0.03
14TGA	5'- GGAGGAGGAGGAGT -3'	0.45±0.09
14CGA	5'- GGAGGAGGAGGAGC -3'	0.53±0.03
14GGA	5'- GGAGGAGGAGGAGG -3'	0.07±0.02
13GA	5'- GGAGGAGGAGGAG -3'	0.15±0.03

B

5' TFO 3'	5'-TGCGCGTG TTCTCCTCCTCCTCC ACCCGCGT-3'**I-31CY** 3'-ACGCGCAC AAGAGGAGGAGGAGG TGGGCGCA-5'**I-31GR**	K_D(μM)
I-14GA	5'- AGAGGAGGAGGAGG -3'	0.11±0.03
I-14TGA	5'- TGAGGAGGAGGAGG -3'	0.11±0.09
I-14CGA	5'- CGAGGAGGAGGAGG -3'	0.10±0.05
14GGA	5'- GGAGGAGGAGGAGG -3'	0.07±0.04
I-13GA	5'- GAGGAGGAGGAGG -3'	0.09±0.02

[a] Values of K_d were calculated as described in Materials and Methods. The mean value of 3−5 different experiments is reported.

those in the first system (31Y/31R), except the 13-nt TFOs (13GA and I-13GA). For instance, the I-12GA bound to I-31Y/31R duplex 5-fold more tightly than the 12GA bound to 31-Y/31R duplex. It was noted that these two TFOs shared a common 10-nt core sequence 5′AGGAGGAG-GAGA3′, and differed only by the position of two Gs (at the 3′ end for the former, or at the 5′ end for the latter). The similar binding affinity of the 13-nt TFOs contrasts with that of other TFOs. It seems that the difference could originate from the presence of a G at the 3′ end in both 13-nt TFOs.

These data strongly suggested that the position of Gs in the (G,A)-containing TFOs governs the stability of triplex. It is known that a C·GxG triplet is more stable than a T·AxA triplet (*6*, *24*), and this might explain the sequence effect observed in this study. To further check this assumption, two other comparative studies were carried out (Tables 2 and 3). They involved mismatched base triplets either at the 5′ or at the 3′ end. Since the mismatched triplets exhibited weaker binding strength than matched triplets, they were used as internal probes in order to delineate the sequence effect on triple helix formation.

Effect of End-Mismatch on Triplex Formation. The two symmetry-related duplexes studied above (31Y/31R and I-31Y/31R) were used with a set of four 14-nt long (G,A)-containing TFOs. These TFOs are derived from the 13GA or I-13GA by addition of one base (A,T,C, or G) at the 3′ end or at the 5′ end, respectively (Table 2). As expected, the K_d values of the 14CGA and 14GGA were significantly higher than those of the 14GA and 14TGA, because the triplexes formed with the 14CGA and the 14GGA involved a mismatched triplet at the 3′ end of TFOs, T·AxC and T·AxG, respectively, whereas those formed with the 14GA and the 14TGA did not contain any mismatched triplet (Table 2A). It came up that a reverse Hoogsteen hydrogen-bonded T·AxT base triplet at the 3′ end contributed to a more stable triplex than its T·AxA analogue; and a mismatched T·AxG triplet had a less destabilizing effect than a mismatched T·AxC triplet at the 3′ end. However, the K_d values of the 14-nt TFOs were higher than that of the 13GA in any case (Table 2A).

An opposite behavior was observed in the system (I-31Y/31R) with reversed polarity. All the 14-nt TFOs had similar K_d values which were slightly lower than that of the I-13GA (Table 2B). It seems that the triplexes formed with the I-14CGA and the 14GGA were slightly destabilized as compared with those formed with the I-14GA and the I-14TGA due to the presence of the mismatched T·AxC and T·AxG triplets, respectively.

A new pair of symmetry-related target duplexes was used in which one T·A base pair facing the terminal base of TFOs either at the 3′ or at the 5′ end was replaced by a C·G base pair. In this case, only the 14GGA can form 14 base triplet-long triplexes without any mismatch on both target duplexes due to its symmetric sequence, whereas the other 14-nt (G,A)-containing TFOs introduced a mismatch either at the 3′ end or at the 5′ end of TFOs in the 31CY/31GR and the I-31CY/31GR systems, respectively (Table 3). As observed above, at the 3′ end of TFOs, the presence of any mismatch destabilized triplexes by about 7-fold in the K_d as compared to the perfect triplex formed with the 14GGA (Table 3A). In addition, the triplex formed with 14GGA was about 2-fold more stable than that formed with the 13GA. This has to be compared with the triplexes formed with the 14GA or the 14TGA which were about 2−3-fold less stable than that formed with the 13GA (Table 2A). In contrast, the triplexes containing a mismatch at the 5 end showed only a moderate destabilization which was about 1.5-fold in the K_d values as compared to the perfect triplex formed with the 14GGA (Table 3B). In this case, the value of the 14GGA was slightly lower than that of the I-13GA.

Taken all the observations together, it consistently emerged that the binding strength of base triplet formed at the 3′ end of TFOs plays a determining role in triple-helix formation.

DISCUSSION AND CONCLUSION

Self-association of oligonucleotides containing (GA)-repeats has previously been reported in the literature. These (G,A)-containing oligonucleotides can form either a parallel-stranded duplex (*36*) or a intramolecular antiparallel-stranded duplex (*47*) or a G_4-quadruplex by dimerization of two hairpin duplexes (*45, 46*). The competition of these self-associated structures with oligonucleotide-directed triplex formation has also been described (*27*). In the current study, it is shown that the oligonucleotides containing (GGA)- or (AGG)-repeats are also prone to self-association, especially in the presence of the divalent cation Mg^{2+}. The pattern of concentration-dependent gel mobility and CD spectra of these self-associated complexes is reminiscent of that observed in parallel-stranded homoduplexes formed by (GA)-repeat oligomers (*36*). Mixing experiments with the oligonucleotides 15GA and $15GAT_7$ confirmed the formation of a dimeric complex. Given the short length of the studied oligomers (13−15 nt) and the fast kinetic behavior, it is unlikely that the self-associated complexes involve G_4-quadruplex with two short hairpin duplexes (*45, 46*). Other possible structures involving G-tetrads (*50*) have not been detected even at high concentrations of oligonucleotide, provided the stock solutions were free of NaCl or KCl. The melting temperatures of the self-associated complexes of oligonucleotides containing (GGA)- or (AGG)-repeats were in the temperature range of 25−33 °C (at 1.5 μM concentration). Therefore, the self-association of these TFOs can effectively compete with triple helix formation even at 37 °C and prevent 100% of triplex formation at high oligonucleotide concentration. The higher the concentration of these (G,A)-containing TFOs, the more TFOs are trapped into self-associated complexes. Therefore, this should be taken into account in order to assess the ability of TFOs containing (GA)- and (GGA)- or (AGG)-repeats to form triple helix.

Consequently, triplex formation was investigated by gel retardation assays under the conditions where the self-association of the (G,A)-containing oligonucleotides did not significantly compete with the process of triplex formation. The relative binding affinity of various TFOs containing (GGA)-/(AGG)-repeats was measured (Table 1). Triplex formation was further confirmed by DNase-I footprinting experiments. It should be noted that UV absorption spectroscopy failed to evidence triplex formation with the (G,A)-containing oligonucleotides; the melting curve (absorbance at 260 nm versus temperature) did not show, under our experimental conditions, any transition other than those corresponding to the melting of the target duplex and the self-associated TFOs. Triple helix formation without hypochromicity has already been described in a few cases (*51, 52*). The self-association of TFOs containing (GGA)- or (AGG)-repeats might hide the duplex-to-triplex transition. On the other hand, the triplex might be very stable so that its transition is hidden by that of the duplex as it has been reported in a number of studies (*28, 31, 32, 53*−*57*). However, the last case does not likely occur in the present study because the measured binding affinities of TFOs were not high enough to expect that triplex dissociation occurs at the same temperature as a 31-bp duplex.

Three-stranded structures have been described which do not correspond to canonical triple helices but contain a D-loop, involving a single-strand oligopyrimidine and a purine·purine parallel homoduplex (*30*). In the current study, the formation of such an unusual complex was ruled out since the assays carried out using both chemical and enzymatic probes (OsO_4 and nuclease P1) failed to provide evidence of any single-stranded sites (data not shown).

What unexpectedly emerged from the present work is that, in one system (31Y/31R), it was not the longest TFO, 15GA, which formed the more stable triplex but rather the 13-nt long TFO, 13GA, with a 5-fold higher affinity as compared to the 15GA (Table 1A). On the other hand, in the other system (I-31Y/31R, in which all sequences were reversed with respect to the 31Y/31R system), the longer the TFO, the more stable is the triplex (Table 1B), as usually observed in the interactions between nucleic acids. It has to be pointed out that all the TFOs shared a common 5′ end but differed at the 3′ end in the first system, whereas they have a common 3′ end and a different 5′ end in the second system.

If only the first three bases at the 3′ end of TFOs are considered, it turns out that the binding affinity of the TFOs with 3′-GGA base sequence (I-13GA, I-14GA, and I-15GA) is quite similar to that of the TFO which starts with 3′-GAG (13GA), and significantly higher than those with 3′-AGA (14GA) and 3′-AAG (15GA). It was observed that the addition of a single G at the 3′ end of the 12GA (13GA) provided more than 10-fold triplex stabilization, whereas the same addition at the 5′ end of the I-12GA (I-13GA) only doubled the triplex stability (Table 1). On the other hand, the addition of an A at the 3′ end of the 13GA (14GA) destabilized 3-fold the triplex (Table 1A), whereas at the 5′ end (I-14GA), it slightly stabilized the triplex (Table 1B). The presence of two T·AxA triplets at the 3′ end of the TFO (15GA compared to 13GA) further destabilized the triple-helix, whereas at the 5′ end a higher stabilization was achieved (I-15GA compared to I-13GA). It should be noted that other TFO analogues containing Gs and Ts instead of Gs and As exhibited similar characteristics (data not shown). This observation suggests a general sequence effect for (G,A)- and (G,T)-containing TFOs.

Further studies involving mismatched base triplets (Tables 2 and 3) showed that the presence of a mismatched triplet at the 3′ end of TFOs caused significant triplex destabilization, whereas the same mismatches at the 5′ end of TFOs had only marginal effects on triplex stability. Even the matched T·AxA and T·AxT base triplets (which have weaker binding strength than the C·GxG triplet) at the 3′ end exhibited notable triplex destabilization as compared to no triplet at all (13GA).

Taken into account the observed sequence effect at both 3′ and 5′ end, it appears that the striking differences in binding affinity of the various TFOs highlight the critical importance of bases (or base triplets) located at the 3′ end of TFOs (the 5′ end of the oligopurine-containing strand since the (G,A)-containing TFOs bound through antiparallel reverse Hoogsteen hydrogen bonds) which determines the affinity of TFOs toward the target sequences. We hypothesizes that the 3′ end of TFOs is likely involved in the nucleation step of triplex formation, i.e., the nucleation

preferentially proceeds in the 5′→3′ direction along the target oligopurine strand.

Cheng and van Dyke (*19*) have already observed length and sequence effects on intermolecular (G,T)-motif triple-helix formation. They found that longer oligonucleotides could be less stable than shorter ones and that extension and point mutations at the 3′ end of TFOs had a consistently greater effect on triplex stability than changes at the 5′ end. They also found using a SELEX method that the selected DNA duplexes for the recognition of a (G,T)-containing oligonucleotide via antiparallel triple-helix formation had an identical sequence of 13 bases at the 3′ end, and a substantial drop in affinity was observed for sequences with only 12 bases of homology at the 3′ end (*58*). Cassidy et al. had also reported similar sequence effect with (G,T)-containing TFOs (*59*, *60*).

In summary, previously published data and our present results demonstrate that there is an asymmetric sequence effect on purine-motif triplex formation. These results, although not completely conclusive, are consistent with the hypothesis that 3′ end of TFOs is deeply involved in the nucleation step of the process of triple helix formation. Further kinetic studies will be required to fully elucidate the mechanism of triplex formation.

ACKNOWLEDGMENT

We thank Dr. J. L. Mergny, J. Lacoste, J. C. François, T. de Bizemont, and C. Giovannangeli for their helpful suggestions, and C. Marchand and L. Perrouault for helpful advice in footprinting experiments.

REFERENCES

1. Felsenfeld, G., Davies, D. R., and Rich, A. (1957) *J. Am. Chem. Soc. 79*, 2023−2024.
2. Le Doan, T., Perrouault, L., Praseuth, D., Habhoub, N., Decout, J.-L., Thuong, N. T., Lhomme, J., and Hélène, C. (1987) *Nucleic Acids Res. 15*, 7749−7760.
3. Moser, H. E., and Dervan, P. B. (1987) *Science 238*, 645−650.
4. François, J. C., Saison-Behmoaras, T., Thuong, N. T., and Hélène, C. (1989) *Biochemistry 28*, 9617−9619.
5. Maher, L. J., III, Wold, B., and Dervan, P. B. (1989) *Science 245*, 725−730.
6. Cooney, M., Czernuszewicz, G., Postel, E. H., Flint, S. J., and Hogan, M. E. (1988) *Science 241*, 456−459.
7. Duval-Valentin, G., Thuong, N. T., and Hélène, C. (1992) *Proc. Natl. Acad. Sci. U.S.A. 89*, 504−508.
8. Maher, L. J., III, Dervan, P. B., and Wold, B. (1992) *Biochemistry 31*, 70−81.
9. Ing, N. H., Beekman, J. M., Kessler, D. J., Murphy, M., Jayaraman, K., Zendegui, J. G., Hogan, M. E., O'Malley, B. W., and Tsai, M. J. (1993) *Nucleic Acids Res. 21*, 2789−2796.
10. Grigoriev, M., Praseuth, D., Robin, P., Hemar, A., Saison-Behmoaras, T., Dautry-Varsat, A., Thuong, N. T., Hélène, C., and Harel-Bellan, A. (1992) *J. Biol. Chem. 267*, 3389−3395.
11. Giovannangeli, C., Perrouault, L., Escude, C., Gryaznov, S., and Helene, C. (1996) *J. Mol. Biol. 261*, 386-398.
12. Young, S. L., Krawczik, S. H., Matteucci, M. D., and Toole, J. J. (1991) *Proc. Natl. Acad. Sci. U.S.A. 88*, 10023−10026.
13. Havre, P. A., Gunther, E. J., Gasparro, F. P., and Glazer, P. M. (1993) *Proc. Natl. Acad. Sci. U.S.A. 90*, 7879−7883.
14. Sandor, Z., and Bredberg, A. (1994) *Nucleic Acids Res. 22*, 2051−2056.
15. Wang, G., and Glazer, P. M. (1995) *J. Biol.Chem. 270*, 22595−22601.
16. Thuong, N. T., and Hélène, C. (1993) *Angew. Chem., Int. Ed. Engl. 32*, 666−690.
17. Pilch, D. S., Levenson, C., and Shafer, R. H. (1991) *Biochemistry 30*, 6081−6087.
18. Cheng, A.-J., and Dyke, M. W. V. (1993) *Nucleic Acids Res. 21*, 5630−5635.
19. Cheng, A. J., and Vandyke, M. W. (1994) *Nucleic Acids Res. 22*, 4742−4747.
20. Milligan, J. F., Matteucci, M. D., and Martin, J. C. (1993) *J. Med. Chem. 36*, 1923−1937.
21. Durland, R. H., Kessler, D. J., Gunnell, S., Duvic, M., Pettitt, B. M., and Hogan, M. E. (1991) *Biochemistry 30*, 9246−9255.
22. Beal, P. A., and Dervan, P. B. (1991) *Science 251*, 1360−1363.
23. Vasquez, K. M., Wensel, T. G., Hogan, M. E., and Wilson, J. H. (1995) *Biochemistry 34*, 7243−7251.
24. Sun, J. S., de Bizemont, T., Duval-Valentin, G., Montenay-Garestier, T., and Hélène, C. (1991) *C. R. Acad. Sci. Paris, Sér. III 313*, 585−590.
25. Bizemont, T. d., Duval-Valentin, G., Sun, J.-S., Bisagni, E., Garestier, T., and Hélène, C. (1996) *Nucleic Acids Res. 24*, 1136−1143.
26. Roy, C. (1993) *Nucleic Acids Res. 21*, 2845−2852.
27. Noonberg, S. B., Francois, J. C., Garestier, T., and Helene, C. (1995) *Nucleic Acids Res. 23*, 1956−1963.
28. Svinarchuk, F., Monnot, M., Merle, A., Malvy, C., and Fermandjian, S. (1995) *Nucleic Acids Res. 23*, 3831−3836.
29. Popa, L. M., Schutz, H., Winter, S., Kittler, L., and Lober, G. (1996) *Biochem. Mol. Biol. Int. 38*, 285−295.
30. Mishima, Y., Suda, T., and Kominami, R. (1996) *J. Biochem. Tokyo 119*, 805−810.
31. Alunni-Fabbroni, M., Pirulli, D., Manzini, G., and Xodo, L. E. (1996) *Biochemistry 35*, 16361−16369.
32. Svinarchuk, F., Paoletti, J., and Malvy, C. (1995) *J. Biol. Chem. 270*, 14068−14071.
33. Hud, N. V., Smith, F. W., Anet, F. A. L., and Feigon, J. (1996) *Biochemistry 35*, 15383−15390.
34. Kang, C., Zhang, X., Ratliff, R., Moyzis, R., and Rich, A. (1992) *Nature 356*, 126- 131.
35. Wang, Y., and Patel, D. J. (1992) *Biochemistry 31*, 8112−8119.
36. Rippe, K., Fritsch, V., Westhof, E., and Jovin, T. M. (1992) *EMBO J. 11*, 3777−3786.
37. Dolinnaya, N. G., and Fresco, J. R. (1992) *Proc. Natl. Acad. Sci. U.S.A. 89*, 9242−9246.
38. Casasnovas, J. M., Huertas, D., Ortizlombardia, M., Kypr, J., and Azorin, F. (1993) *J. Mol. Biol. 233*, 671−681.
39. Huertas, D., Bellsolell, L., Casasnovas, J. M., Coll, M., and Azorin, F. (1993) *EMBO J. 12*, 4029−4038.
40. Robinson, H., Vanboom, J. H., and Wang, A. H. J. (1994) *J. Am. Chem. Soc. 116*, 1565−1566.
41. Evertsz, E. M., Rippe, K., and Jovin, T. M. (1994) *Nucleic Acids Res. 22*, 3293−3303.
42. Ortizlombardia, M., Eritja, R., Azorin, F., Kypr, J., Tejralova, I., and Vorlickova, M. (1995) *Biochemistry 34*, 14408−14415.
43. Suda, T., Mishima, Y., Asakura, H., and Kominami, R. (1995) *Nucleic Acids Res. 23*, 3771−3777.
44. Suda, T., Mishima, Y., Takayanagi, K., asakura, H., Odani, S., and Kominami, R. (1996) *Nucleic Acids Res. 24*, 4733−4740.
45. Shiber, M. C., Braswell, E. H., Klump, H., and Fresco, J. R. (1996) *Nucleic Acids Res. 24*, 5004−5012.
46. Mukerji, I., Shiber, M. C., Fresco, J. R., and Spiro, T. G. (1996) *Nucleic Acids Res. 24*, 5013−5020.
47. Huertas, D., and Azorin, F. (1996) *Biochemistry 35*, 13125−13135.
48. Lee, J. S. (1990) *Nucleic Acids Res. 18*, 6057−6060.
49. Cantor, C. R., and Schimmel, P. R. (1980) in *Biophysical Chemistry Part III*, Freeman, W. H., and Company, San Francisco.
50. Sen, D., and Gilbert, W. (1988) *Nature 334*, 364−366.
51. Jetter, M. C., and Hobbs, F. W. (1993) *Biochemistry 32*, 3249−3254.
52. Faucon, B., Mergny, J.-L., and Hélène, C. (1996) *Nucleic Acids Res. 24*, 3181−3188.

53. Alunni-Fabbroni, M., Manfioletti, G., Manzini, G., and Xodo, L. E. (1994) *Eur. J. Biochem. 226*, 831−839.
54. Svinarchuk, F., Bertrand, J. R., and Malvy, C. (1994) *Nucleic Acids Res. 22*, 3742−3747.
55. Svinarchuk, F., Debin, A., Bertrand, J. R., and Malvy, C. (1996) *Nucleic Acids Res. 24*, 295−302.
56. Svinarchuk, F., Cherny, D., Debin, A., Delain, E., and Malvy, C. (1996) *Nucleic Acids Res. 24*, 3858−3865.
57. Alunni-Fabbroni, M., Manzini, G., Quadrifoglio, F., and Xodo, L. E. (1996) *Eur. J. Biochem. 238*, 143−151.
58. Hardenbol, P., and Vandyke, M. W. (1996) *Proc. Natl. Acad. Sci. U.S.A. 93*, 2811- 2816.
59. Cassidy, S. A., Strekowski, L., Wilson, W. D., and Fox, K. R. (1994) *Biochemistry 33*, 15338−15347.
60. Cassidy, S. A., Strekowski, L., and Fox, K. R. (1996) *Nucleic Acids Res. 24*, 4133- 4138.

BI9805588